Adaptive Mesh Refinement for Singular Solutions of the Incompressible Euler Equations

Rainer Grauer, Christiane Marliani, and Kai Germaschewski
Institut für Theoretische Physik I, Heinrich-Heine-Universität Düsseldorf, D-40225 Düsseldorf, Germany
(Received 3 December 1997)

The occurrence of a finite time singularity in the incompressible Euler equations in three dimensions is studied numerically using the technique of adaptive mesh refinement. As opposed to earlier treatments, a prescribed accuracy is guaranteed over the entire integration domain. A singularity in the vorticity could be traced down to five levels of refinement which corresponds to a resolution of 2048^3 mesh points in a nonadaptive treatment. The growth of vorticity fits a power law behavior proportional to $1/(T^* - t)$ where T^* denotes the time when the singularity occurs. [S0031-9007(98)06038-4]

PACS numbers: 47.11.+j, 03.40.Gc, 47.10.+g, 47.15.Ki

The question whether the three-dimensional incompressible Euler equations,

$$\partial_t \mathbf{u} + \mathbf{u} \cdot \nabla \mathbf{u} + \nabla p = 0, \qquad \nabla \cdot \mathbf{u} = 0, \quad (1)$$

develop a finite time singularity in the vorticity is still a controversial issue. This is not only a mathematically open issue but may also be relevant for the properties of small scale structures in viscous turbulent flows (see Frisch [1], Chaps. 7 and 9). In the last years, there have been several high-resolution numerical experiments [2–4] studying the possible formation of a finite time singularity. Unfortunately, not all simulations agree in their conclusions. An explanation could be related to the findings in two-dimensional quasigeostrophic flows studied by Constantin, Majda, and Tabak [5]. They found that whether a finite time singularity develops or whether vorticity grows only exponentially in time depends strongly on the geometry of the initial conditions. A similar statement may be relevant for the three-dimensional incompressible Euler equations which could explain why the Taylor-Green vortex used as initial condition in the simulations by Brachet *et al.* [4] shows only exponential growth due to its high degree of symmetry.

The main issue in performing simulations of the three-dimensional incompressible Euler equations is the achieved numerical resolution limited by the available computer resources. The simulations presented in [3,4] use a fixed grid of given resolution. The spatial resolution of 256^3 nodes is impressive documenting the enormous progress in computer resources. In addition, these calculations use spatial symmetries to enlarge the effective resolution. However, this resolution is still too low to conclude about the scaling behavior of a finite time blowup. To overcome this difficulty, Pumir and Siggia [6] used some sort of adaptivity to enlarge the numerical resolution. Their method consists of introducing coordinate transformations such that inside a small box the numerical resolution is sufficient. The drawback of this method is that the flow is not resolved outside the maximum vorticity region, and therefore the global flow loses energy by a factor of 30.

In this Letter, we use a technique of adaptive mesh refinement similar to the method introduced by Berger and Collela [7] for shock hydrodynamics. The application of adaptive mesh refinement to incompressible flows was demonstrated in Friedel, Grauer, and Marliani [8] for two-dimensional magnetohydrodynamics and by Howell and Bell [9] to the two-dimensional Navier-Stokes equations.

The idea of adaptive mesh refinement is very natural. One starts with an initial grid of given resolution (here we chose 64^3 mesh points) and integrates the Euler equations (1) using some appropriate numerical scheme. The numerical resolution is checked after a certain number of time steps: Grid points where local gradients (we use the matrix norm $||\nabla \mathbf{u}||$, so shear and rotational effects are accounted for) exceed a given threshold are marked as critical points, i.e., points where the local numerical resolution is not sufficient. Additionally, the trajectories of these points are estimated using local velocities and used to mark prospective critical points. This enables the grid hierarchy to follow moving structures. Next, the marked points are covered with rectangular grids of finer resolution by an algorithm very similar to that of Berger and Rigoutsos [10] and which was described in Friedel *et al.* [8]. On the grids of the newly built level the spatial discretization length and the time step are reduced by a factor of 2 resulting in no change of the Courant-Friedrichs-Lewy condition. The new grids are filled with data of the vorticity interpolated from the preceding level. This procedure is different from the approach of Howell and Bell [9] where the velocity fields are interpolated. On both levels integration advances until the resolution again becomes locally insufficient. The rebuilding of the grid hierarchy starting with the current level and proceeding on all subsequent levels begins when the above-mentioned criterion is fulfilled, e.g., if local gradients have developed such that the prescribed accuracy is not guaranteed. Next, the points are marked on all grids of each level. On the basis of the resulting lists of critical points new grids are generated. Before they can be filled with data it has to be checked whether they are correctly embedded in grids of the preceding level. If data existed on grids of the same level before

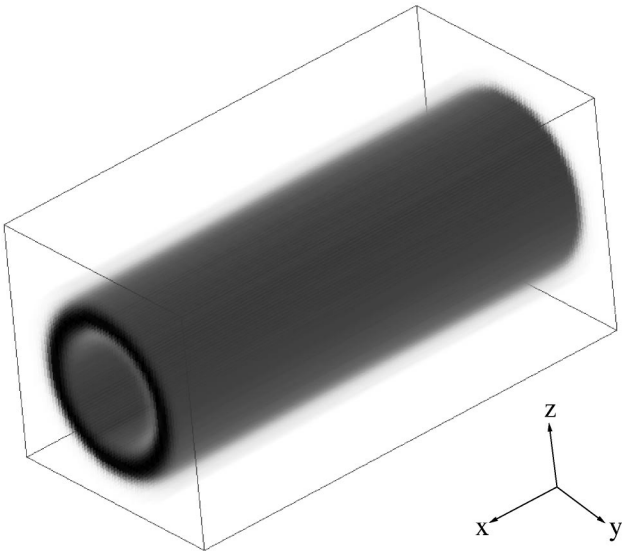

FIG. 1. Volume rendering of $|\boldsymbol{\omega}|$ at time 0.06.

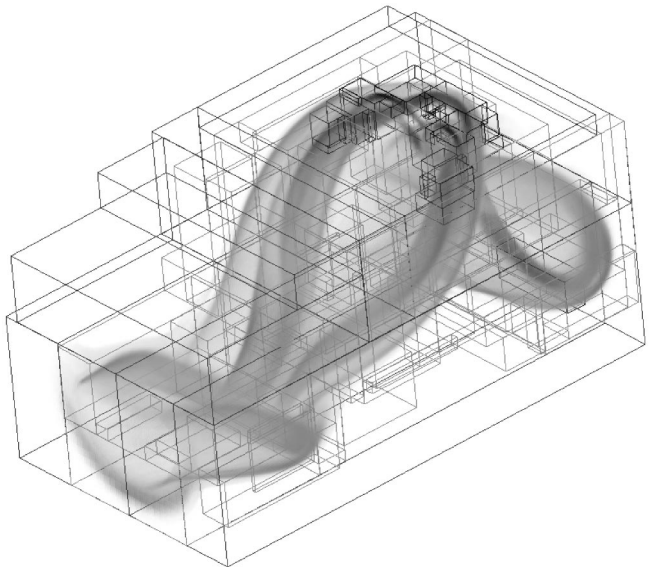

FIG. 3. Volume rendering of $|\boldsymbol{\omega}|$ at time 1.18.

the regridding, these have to be taken instead of the interpolated data.

Having explained the strategy of adaptive mesh refinement, it remains to comment on the integration scheme which is used on all grids involved. It is a projection method combined with second order upwinding as introduced in Bell *et al.* [11].

As the initial condition we used a perturbed cylindrical shear flow which had been introduced by Bell and Marcus [12]. The initial velocity is given by

$$\mathbf{u}_0 = \left(\tanh\left[\frac{(\rho - \sqrt{y^2 + z^2})}{\delta}\right], 0, \epsilon e^{-\beta(x^2+y^2)}\right),$$

with $\rho = 0.15$, $\delta = 0.0333$, $\epsilon = 0.05$, and $\beta = 15$. This represents a hollow-cored vortex tube around the x axis, subject to a Gaussian-shaped perturbation in the z direction. This slight perturbation (characterized by ϵ) breaks the cylindrical symmetry so that only a mirror symmetry with respect to y remains. Figures 1–4 show volume renderings of the absolute value of vorticity for progressing times. Initially, vorticity is concentrated only in the region of shear resulting in a tubular structure. The resolution of the coarsest grid is given by 64^3 mesh points. Figure 1 shows part of the integration domain where the tube of vorticity is covered by one level of refinement. In Fig. 2 the development of a Kelvin-Helmholtz instability is shown which forms from the slight transverse perturbation in the initial condition. At the same time the resolution is automatically

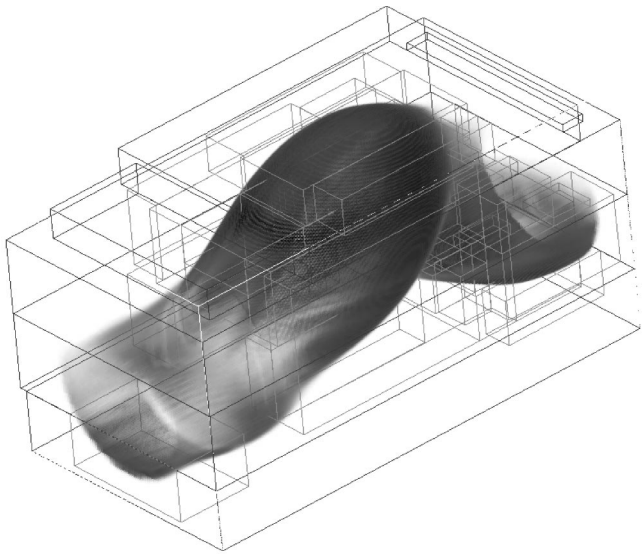

FIG. 2. Volume rendering of $|\boldsymbol{\omega}|$ at time 0.99.

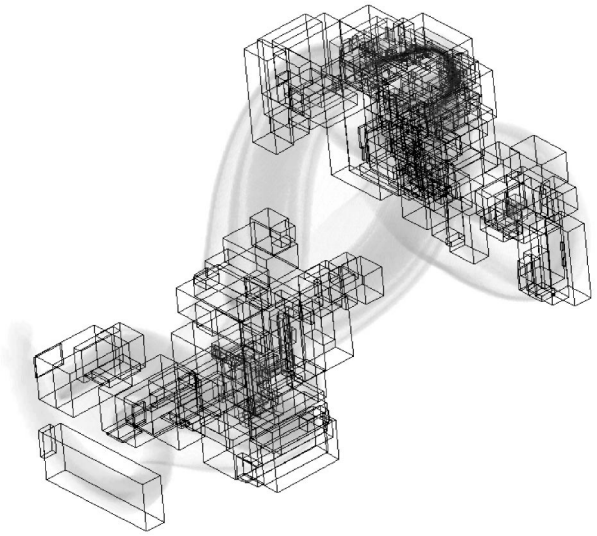

FIG. 4. Volume rendering of $|\boldsymbol{\omega}|$ at time 1.32. Only level 3, 4, and 5 grids are shown.

FIG. 5. Volume rendering of $|\boldsymbol{\omega}|$ at time 1.32.

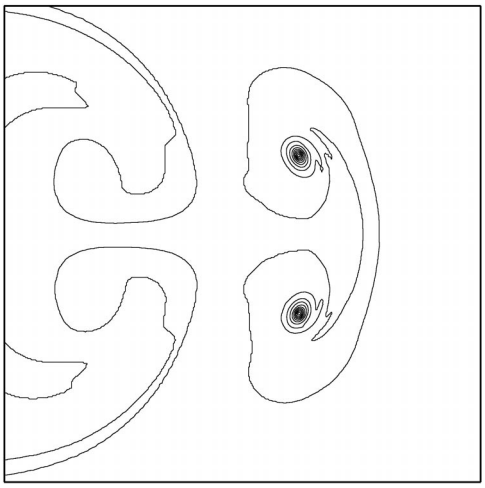

FIG. 7. Two-dimensional cut of $|\boldsymbol{\omega}|$ at time 1.32.

enlarged in those regions where steep gradients develop. Figure 2 shows two levels of refinement corresponding to 256^3 mesh points in a nonadaptive treatment. Figures 3 and 4 show the formation of a hairpinlike structure. This is the region where the finite time singularity occurs. Figures 3 and 4 contain three and five levels (respectively) of refinement corresponding to 512^3 and 2048^3 mesh points. Since the vortex structure in Fig. 4 is hidden by the hierarchically nested grids, we show the same picture without boxes in Fig. 5. The hairpin vortex visible in the upper right part is magnified in Fig. 6. It shows the isosurface of 60% maximum vorticity; in addition, the covering with the finest level is depicted. To demonstrate that the flow is sufficiently resolved we show in Fig. 7 a two-dimensional cut through the hairpin vortex in the y-z plane as a contour plot. Both plots in Fig. 8 are obtained as one-dimensional cuts in the y direction through the maxima of Fig. 7. The absolute value of vorticity is shown as a function of y in units of the finest level's mesh

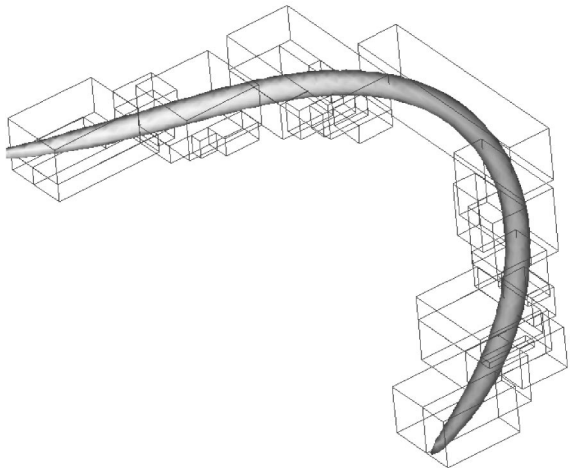

FIG. 6. Hairpin structure at time 1.32.

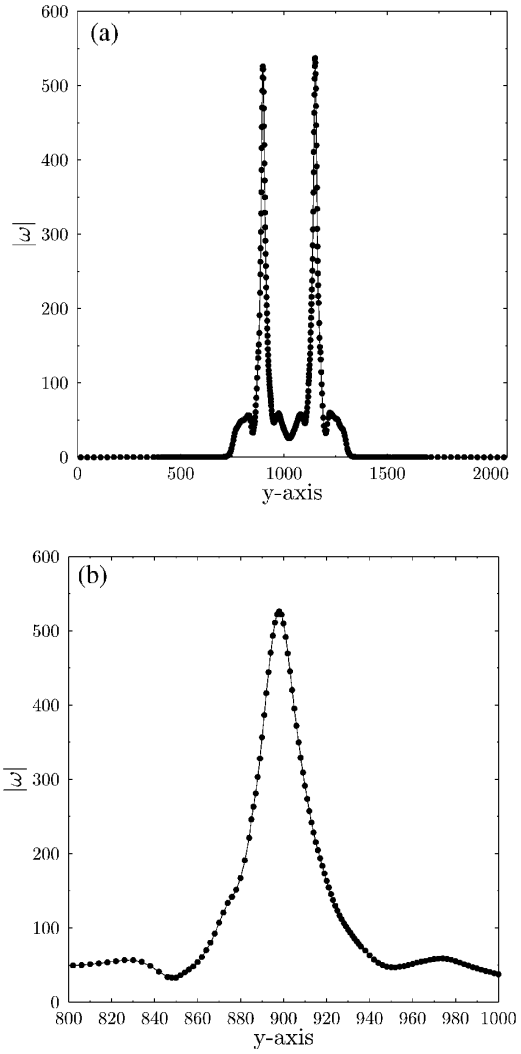

FIG. 8. One-dimensional cuts of $|\boldsymbol{\omega}|$ at time 1.32.

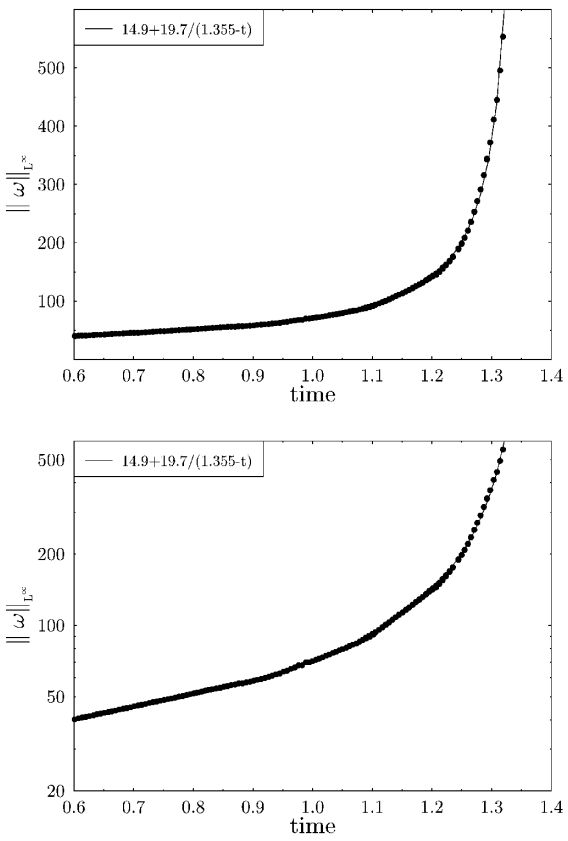

FIG. 9. Growth of vorticity versus time using a linear and a logarithmic y axis, respectively.

spacing. The lower graph shows part of the spatial domain containing only the left peak in the vorticity. One can clearly see that the vorticity peaks are well resolved.

Using a second order upwind scheme has the advantage that one can detect whether the flow is resolved by monitoring the energy conservation. Upwind schemes produce substantial energy dissipation if steep gradients are not sufficiently resolved. Therefore, the conservation of energy is a measure whether the flow is correctly resolved. During the whole calculation the energy is conserved within less than 1%.

It is important to comment on the alignment properties of the flow. In our calculations we found perfect alignment between the eigenvalue corresponding to the middle eigenvalue of the deformation matrix $(\nabla \mathbf{u} + {}^T\nabla \mathbf{u})/2$ and the vorticity vector $\boldsymbol{\omega}$.

In Fig. 9 we show the temporal evolution of the L_∞ norm of the vorticity. The semilogarithmic plot rules out an only exponential growth of vorticity. For comparison we include a fit of the form $a + b/(T^* - t)$. The constant $a = 14.9$ corresponds to the global background vorticity introduced by the shear flow initial condition. This type of blowup is consistent with the result of Beale *et al.* [13] which is a necessary (not sufficient) check whether the simulations produce numerical artifacts.

In conclusion, we have presented numerical simulations which strongly support the existence of a finite time singularity in the vorticity. Using the technique of adaptive mesh refinement, it is possible to reach an effective numerical resolution of 2048^3 mesh points using less than 1% of the resources that would be necessary for a nonadaptive simulation of the same effective resolution. However, many questions remain open; for example, we are not yet able to link our results to the theorem of Constantin, Fefferman, and Majda [14]. This theorem states that for certain *smoothly directed* sets a finite time singularity can be ruled out if the vorticity direction field $\nabla\boldsymbol{\omega}/|\boldsymbol{\omega}|$ is smooth. In addition, one has to understand why the highly symmetric Taylor-Green initial condition does not show a finite time singularity [4], whereas the Kida flow initial condition which possesses even higher symmetry leads to the formation of a finite time singularity [3]. We are currently trying to repeat those initial conditions as well as Kerr's colliding vortex tubes using our adaptive mesh refinement code in order to understand the mechanism for singular vorticity production.

We thank H. Friedel for stimulating discussions and K. H. Spatschek for his continuous support. This work was performed under the auspices of the Sonderforschungsbereich 191.

[1] U. Frisch, *Turbulence* (Cambridge University Press, Cambridge, 1995).
[2] R. M. Kerr, Phys. Fluids A **5**, 1725 (1993).
[3] O. N. Boratav and R. B. Pelz, Phys. Fluids **6**, 2757 (1994).
[4] M. E. Brachet *et al.*, Phys. Fluids A **4**, 2845 (1992).
[5] P. Constantin, A. J. Majda, and E. G. Tabak, Phys. Fluids **6**, 9 (1994).
[6] A. Pumir and E. Siggia, Phys. Fluids. A **2**, 220 (1990).
[7] M. J. Berger and P. Colella, J. Comput. Phys. **82**, 64 (1989).
[8] H. Friedel, R. Grauer, and C. Marliani, J. Comput. Phys. **134**, 190 (1997).
[9] L. H. Howell and J. B. Bell, SIAM J. Sci. Comput. **18**, 996 (1997).
[10] M. Berger and I. Rigoutsos, IEEE Trans. Syst. Man Cybern. **21**, 1278 (1991).
[11] J. B. Bell, P. Colella, and H. M. Glaz, J. Comput. Phys. **85**, 257 (1989).
[12] J. B. Bell and D. L. Marcus, Commun. Math. Phys. **147**, 371 (1992).
[13] J. T. Beale, T. Kato, and A. Majda, Commun. Math. Phys. **94**, 61 (1984).
[14] P. Constantin, C. Fefferman, and A. J. Majda, Commun. Part. Diff. Eq. **21**, 559 (1996).